Plasma physics

2023 winter s. 2/1 , C+Ex

prof. Juraj Glosík, doc. Radek Plašil

- Negative ions in plasma
- Elementary processes: recombination

Negative ions—anions—in plasma

Electronegative plasma
boundary condition for
validity of Bohm criterion

$$\frac{T_e}{T_{\text{anion}}} \lesssim 10$$

$$\frac{n_{\text{anion}}}{n_e} \lesssim 3$$

$$\frac{n_{\text{anion}}}{n_e} \approx \sqrt{\frac{T_e}{T_{\text{anion}}}}$$

$$\frac{n_{\text{anion}}}{n_e} \lesssim 10$$

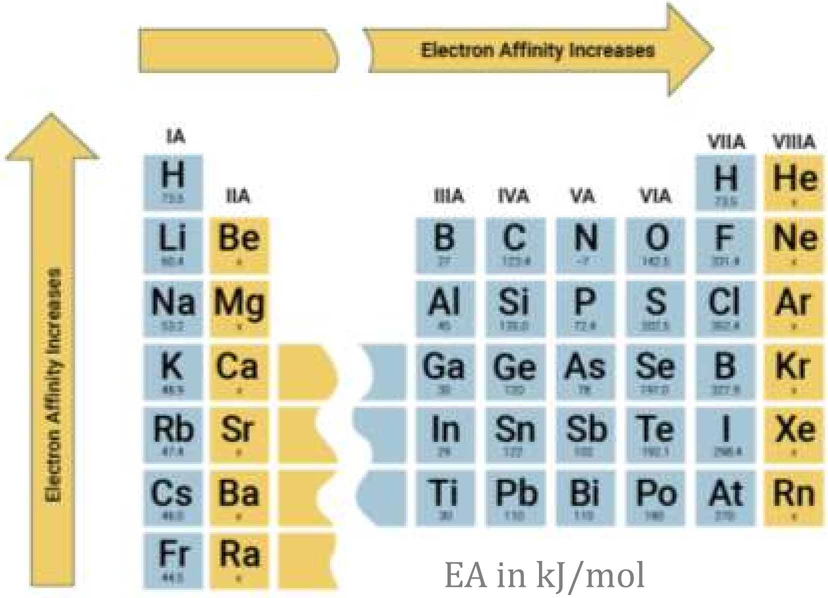

EA in kJ/mol

Species	Electron Affinity "EA"
O_2	0.45 eV
H	0.75 eV
C	1.3 eV
O	1.5 eV
Cl	3.6 eV
C_6H	3.8 eV

McCarthy M. C. et al. *ApJ* 652 (2006) L141
doi: 10.1086/510238

"Electron Affinity of The Elements" Published on Jun 19, 2021.
https://breakingatom.com/learn-the-periodic-table/electron-affinity-of-the-elements

https://webbook.nist.gov/chemistry/ea-ser/

Formation of anions in plasma

- Ion-pair formation

$$H_2 + h\nu \rightarrow H^- + H^+$$

$$CH_4 + h\nu \rightarrow H^- + CH_3^+$$

Maximum cross sections
≈ 20 eV

- Radiative electron attachment

$$H + e^- \rightleftarrows (H^-)^* \rightarrow H^- + h\nu$$

$k = 3{\cdot}10^{-16}\ cm^3\ s^{-1}$

at 300 K

$$C_6H + e^- \rightleftarrows (C_6H^-)^* \rightarrow C_6H^- + h\nu$$

$k = 6{\cdot}10^{-8}\ cm^3\ s^{-1}$

- Dissociative attachment

$$CH_4 + e^- \rightarrow CH_2^- + H_2$$

$$HCN + e^- \rightarrow CN^- + H$$

Destruction of anions

- Photodetachment

$$O^- + h\nu \rightarrow O + e^-$$

- Associative detachment

$$H^- + H \rightarrow H_2 + e^-$$

$$O^- + H_2 \rightarrow H_2O + e^-$$

- Cation-Anion recombination

$$HCO^+ + H^- \rightarrow CO + H_2$$

- Electron detachment in collision

$$H^- + H \rightarrow H + H + e^-$$

$$H^- + e^- \rightarrow H + e^- + e^-$$

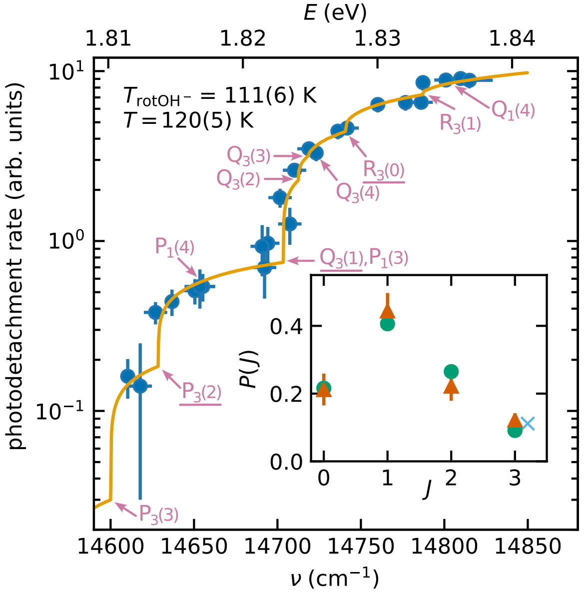

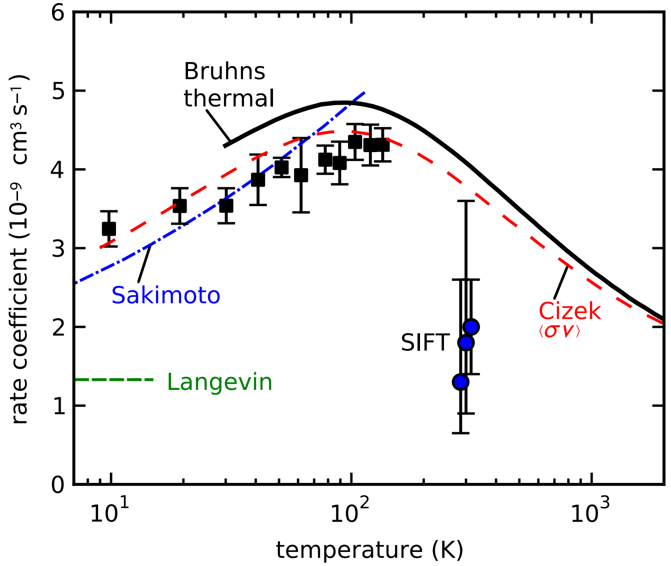

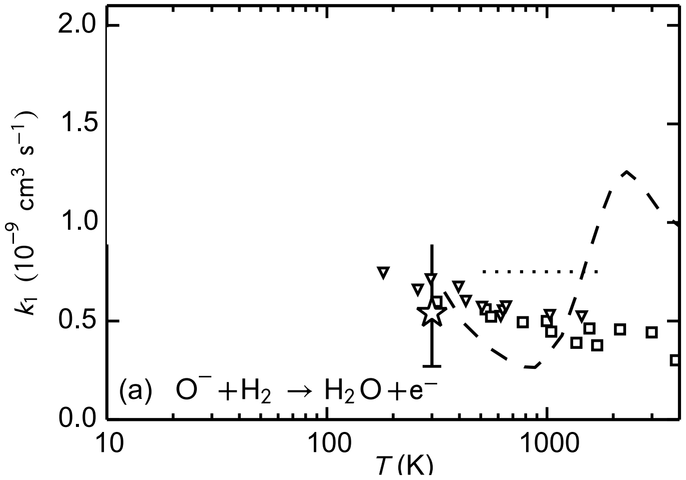

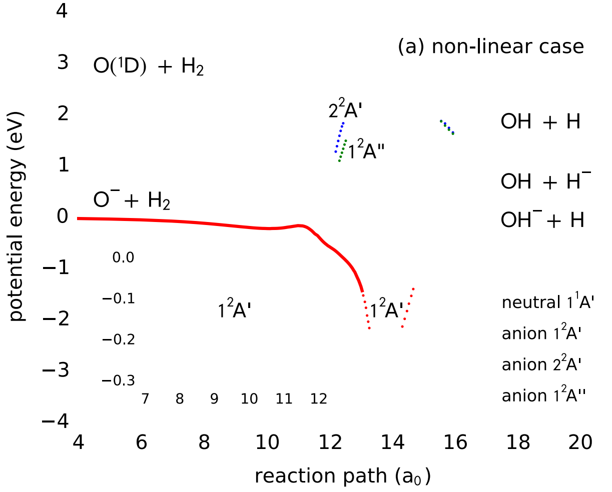

Solar opacity

Photosphere of Sun 6500 to 4200 K
the energy is transferred by radiation, convection is stopped
photon mean free path 1 to 100 km

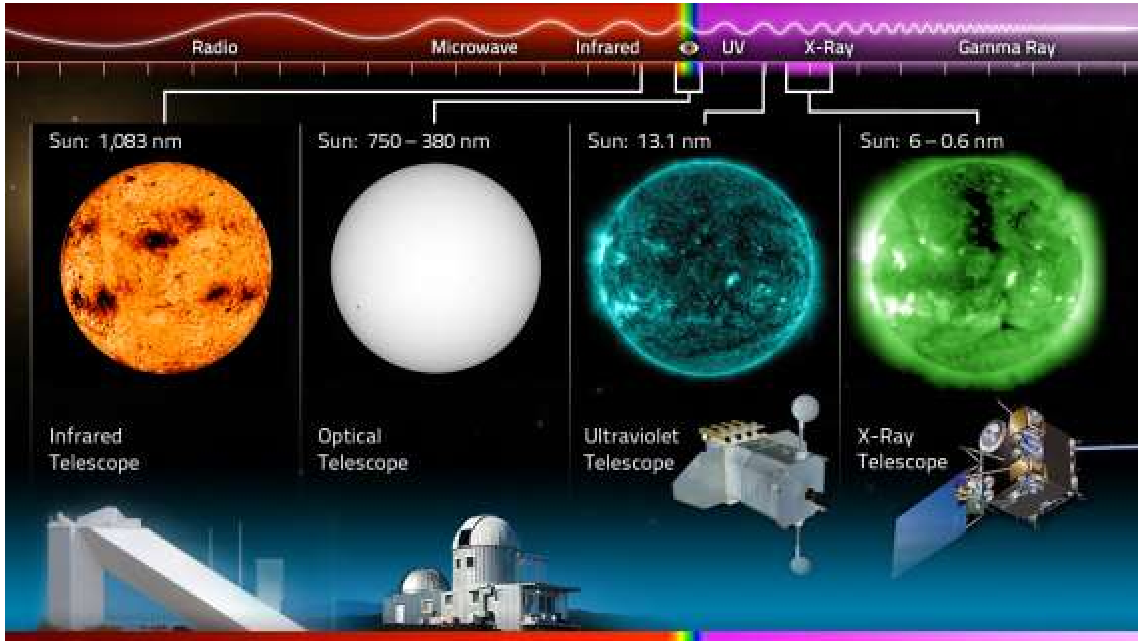

Multiwavelength Astronomy project
ecuip.lib.uchicago.edu/multiwavelength-astronomy/astrophysics/02.html

Transitions

- bond-bond transitions

$$h\nu + \mathrm{H}(n_1) \rightarrow \mathrm{H}(n_2 > n_1)$$

- free-free transitions
  inverse Bremsstrahlung

$$h\nu_1 + e^- + \mathrm{H}^+ \rightarrow h\nu_2 + e^- + \mathrm{H}^+$$

- bond-free transition

$$h\nu + \mathrm{H}(n) \rightarrow \mathrm{H}^+ + e^-$$

$$n = 1 \Rightarrow 13.6\ \mathrm{eV};\ n = 2 \Rightarrow 3.4\ \mathrm{eV}$$

visible 1.6 — 3.3 eV

$$h\nu + \mathrm{H}^- \rightarrow \mathrm{H} + e^-$$

$$n = 1 \Rightarrow 0.75\ \mathrm{eV}$$

electron affinity

Sun

$$\frac{[\mathrm{H}^-]}{[\mathrm{H}]} \approx 10^{-7} \qquad \frac{[\mathrm{H}(n \geq 3)]}{[\mathrm{H}]} \approx 10^{-9}$$

The continuum radiation is mostly formed by bond-free transitions of the anion H⁻.
It is very similar to the black body radiation with a maximum at λ = 500 nm.

Recombination of positive ions

Recombination rate coefficient $\alpha \equiv k_{\mathrm{recombination}}$

$$\zeta(t) = \frac{n_\mathrm{i}}{n_e}$$

Net recombination loss due to
one type of cation "i"—for example O_2^+

$$\frac{\mathrm{d}n_e}{\mathrm{d}t} = -\alpha\, n_\mathrm{i} n_e \quad = -\alpha\, \zeta(t) n_e^2$$

Afterglow plasma   Recombination and Diffusion losses

In case of one dominant ion species
$\zeta(t) = 1$

$$\frac{\mathrm{d}n_e}{\mathrm{d}t} = -\alpha\, n_e^2 - D_\mathrm{a}\nabla^2 n_e$$

$$D_\mathrm{a}\nabla^2 n_e = \frac{D_\mathrm{a}}{\Lambda^2} n_e = \frac{1}{\tau_\mathrm{D}} n_e$$

$$\frac{\mathrm{d}n_e}{\mathrm{d}t} = -\alpha\, n_e^2 - \frac{n_e}{\tau_\mathrm{D}}$$

$$\frac{\mathrm{d}n_e}{\mathrm{d}t} = -\alpha\, n_e^2$$

$$\frac{1}{n_e(t)} = \frac{1}{n_e(t_0)} + \alpha(t - t_0)$$

$$\frac{1}{n_e(t)} = \frac{1}{n_e(t_0)} \exp\left(\frac{t}{\tau_\mathrm{D}}\right) + \alpha\, \tau_\mathrm{D}\left[\exp\left(\frac{t}{\tau_\mathrm{D}}\right) - 1\right]$$

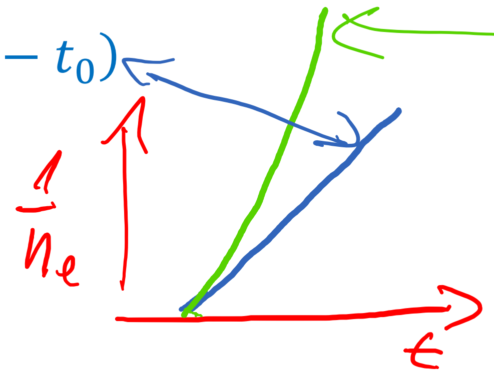

Recombination of positive ions

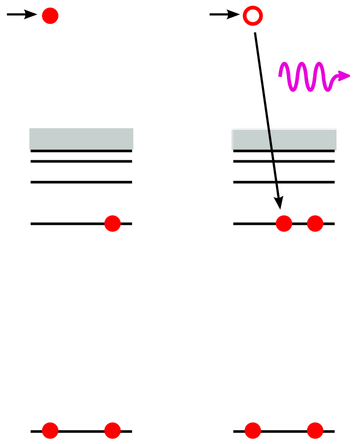

$\alpha \approx 10^{-10}\ \mathrm{cm^3\,s^{-1}}$

$$A^+ + e^- \xrightarrow{\alpha_{\text{radiative}}} A + h\nu \qquad H^+ + e^- \xrightarrow{\alpha_{\text{radiative}}} H + h\nu$$

$$AB^+ + e^- \xrightarrow{\alpha_{\text{radiative}}} AB + h\nu$$

$$A^+ + e^- \underset{\text{resonant}}{\xrightarrow{\alpha_{\text{dielectronic}}}} A + h\nu \qquad O^{7+} + e^- \xrightarrow{\alpha_{\text{dielectronic}}} O^{6+} + h\nu$$

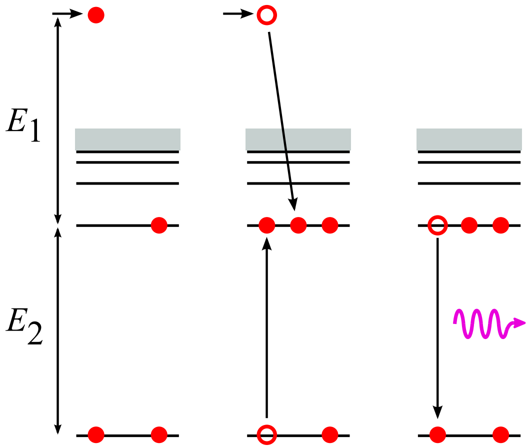

$\alpha \approx 10^{-10} - 10^{-7}\ \mathrm{cm^3\,s^{-1}}$

$$AB^+ + e^- \xrightarrow{\alpha_{\text{dissociative}}} A + B \qquad O_2^+ + e^- \xrightarrow{\alpha_{\text{dissociative}}} O + O$$

Nakamura N. *J. Phys. B* 49 (2016) 212001.
doi: 10.1088/0953-4075/49/21/212001

Dissociative recombination of positive ions

Direct recombination

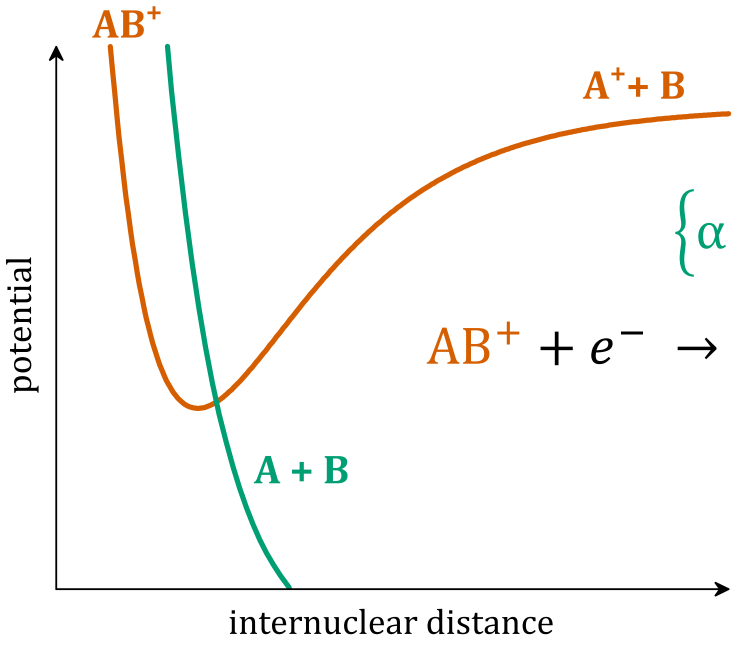

$$\left\{\alpha \sim T_e^{-1/2}\right\}$$

$$AB^+ + e^- \rightarrow A + B$$

Indirect recombination

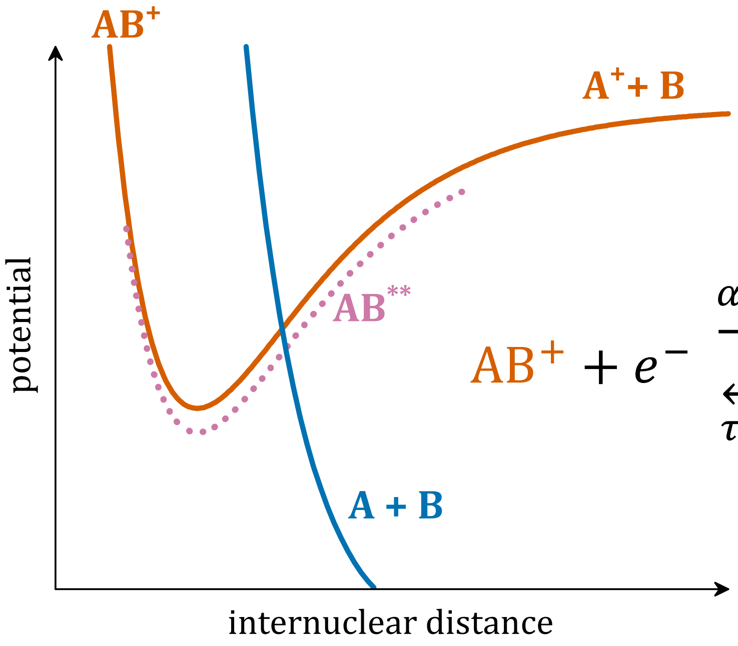

$$\left\{\alpha \sim T_e^{-3/2}\right\}$$

$$AB^+ + e^- \underset{\tau_{\text{autoioniz.}}}{\overset{\alpha_{\text{formation}}}{\rightleftarrows}} AB^{**} \rightarrow A + B$$

Rydberg states

$$r_{\text{orbital}} = 4\pi\varepsilon_0 \frac{n^2\hbar^2}{q^2 m}$$

Bardsley J. N., Biondi M. A. 1970. Advances in atomic and molecular physics. In: DR Bates, editors. New York: Academic Press. pp 1–57.

$$Ar^+ + e^- + M \xrightarrow{\alpha_{\text{ternary}}} Ar + M$$

$$Ar^+ + e^- + e^- \xrightarrow{\alpha_{\text{ternary}}} Ar + e^-$$ Collisional Radiative Recombination

$$Ar^+ + e^- + He \xrightarrow{\alpha_{\text{ternary}}} Ar + He$$ Neutral Assisted Recombination

Example of dissociative recombination O_2^+

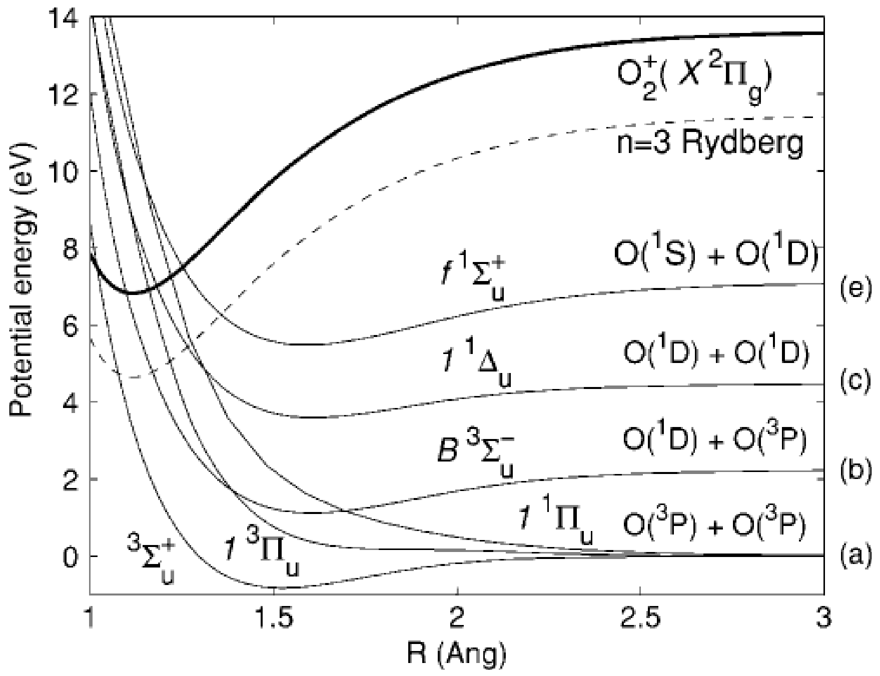

FIG. 1. Schematic of the diabatic potential curves relevant for the DR of O_2^+. The dissociation limits connected with each valence capture state are given on the right. The labels (a)–(c), and (e) refer to Eqs. (1a)–(1c) and (1e), respectively.

Petrignani A. et al. *J. Chem. Phys.* 122 (2005) 23431
doi: 10.1063/1.1937388.

$$O_2^+(X^2\Pi_g, v=0) + e^- \xrightarrow{\alpha_{\rm diss}} O(^3P) + O(^3P) + 6.7\ \text{eV}$$
$$\longrightarrow O(^3P) + O(^1D) + 5.0\ \text{eV}$$
$$\longrightarrow O(^1D) + O(^1D) + 3.0\ \text{eV}$$
$$\longrightarrow O(^3P) + O(^1S) + 2.8\ \text{eV}$$
$$\longrightarrow O(^1D) + O(^1S) + 0.8\ \text{eV}$$

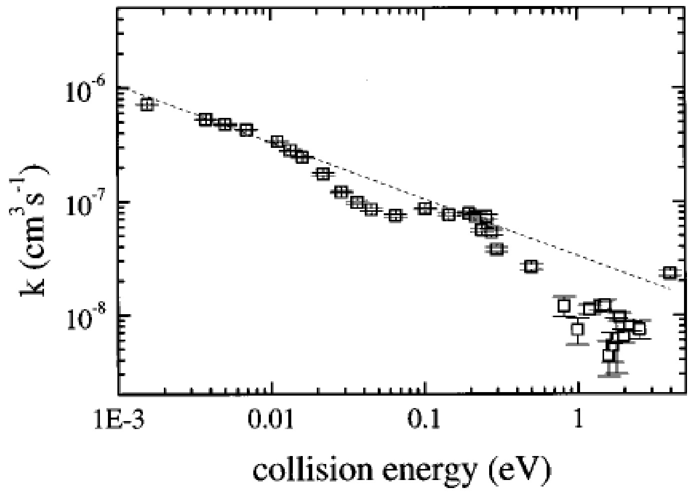

FIG. 2. DR rate coefficient k as a function of electron collision energy from 1 meV to 5 eV. Statistical errors are shown at the 1σ level. The dotted line shows the threshold $E^{-1/2}$ behavior. Both the rate coefficient and the energy are shown on a logarithmic scale.

Peverall R. et al. *J. Chem. Phys.* 114 (2001) 6679
doi: 10.1063/1.1349079

DR without curve crossing

Tunneling dissociative recombination

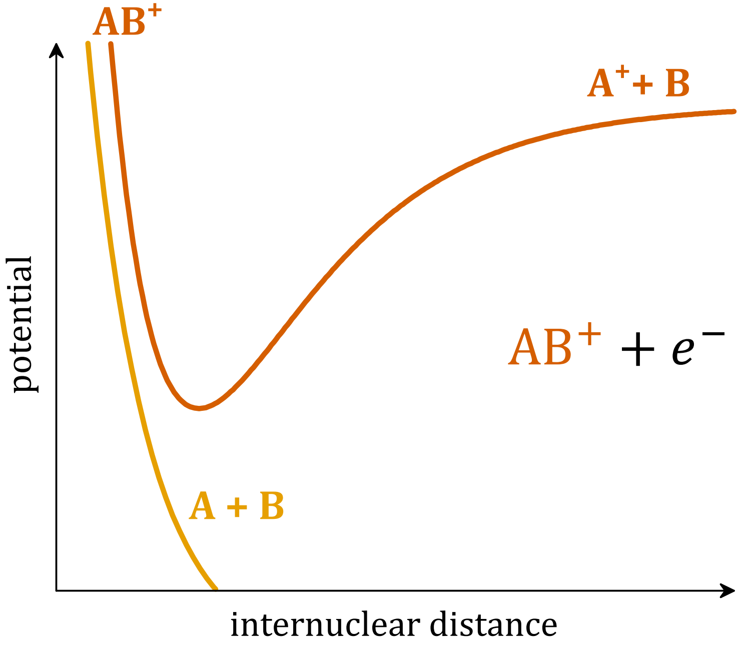

$$AB^+ + e^- \rightarrow A + B$$

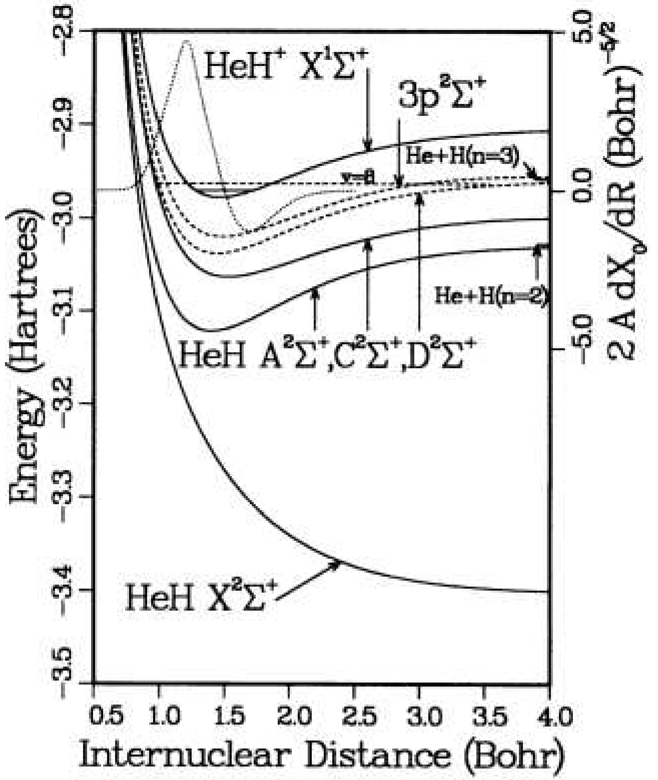

FIG. 1. The calculated HeH dissociative potential-energy curves (solid lines), the $n = 3$ Rydberg states (dashed lines), and the HeH^+ ground state (solid line) with the $v = 0$ level are shown. The $v = 8$ resonance level of the $D\,^2\Sigma^+$ state is shown as the dashed line. The dotted line shows the product, $2A(R)d\chi_0/dR$, with its ordinate axis on the right.

Steven L. Guberman S. L. *Phys. Rev. A* 49 (1994) R4277.
doi: 10.1103/PhysRevA.49.R4277

DR of HeH^+

Astrophysical detection of the helium hydride ion HeH^+

Rolf Güsten[1]*, Helmut Wiesemeyer[1], David Neufeld[2], Christophe Risacher[1,5] & Jürgen Stutzki[3]

Güsten R. et al. *Nature* 568 (2019) 357.
doi: 10.1038/s41586-019-1090-x

Reaction	Rate coefficient $[cm^3\ s^{-1}]$	Notes
$He^+ + H \rightarrow HeH^+ + h\nu$	1.4×10^{-16}	1
$HeH^+ + e \rightarrow He + H$	$3.0 \times 10^{-10}\ (T/10^4\ K)^{-0.47}$	2
$HeH^+ + H \rightarrow He + H_2^+$	$1.2 \times 10^{-9}\ (T/10^4\ K)^{-0.11}$	3

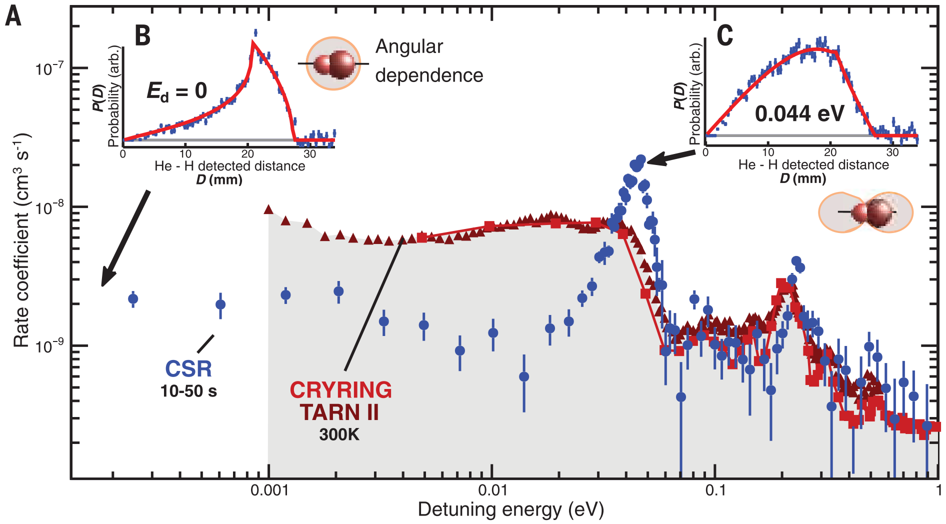

Novotný O. et al. *Science* 365 (2019) 676.
doi: 10.1126/science.aax5921

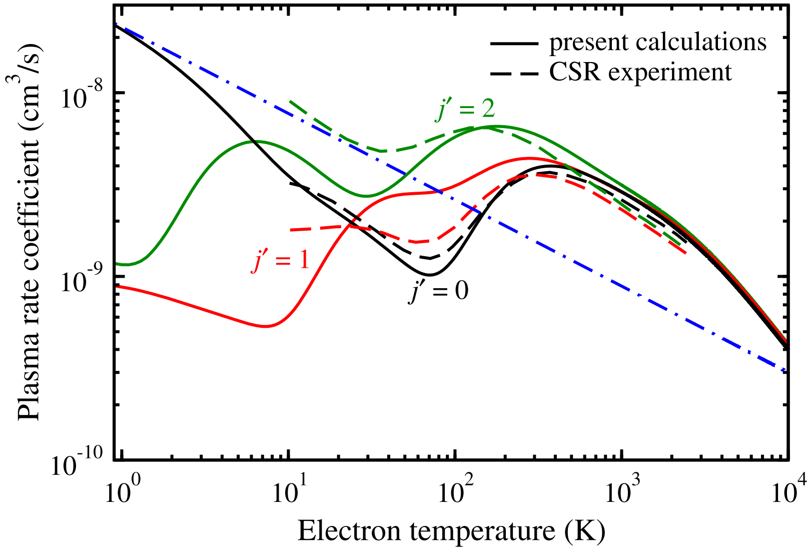

FIG. 5. Plasma rate coefficients are shown for different initial rotational states $j' = 0, 1, 2$. The solid curves result from the present theory, while the dashed curves are taken from the experiment at the CSR [4]. The dot-dashed line represents data employed by Guesten *et al.* [1] in their chemistry kinetics simulations of NGC 7027.

Čurík R. et al. *Phys. Rev. Lett.* 124 (2020) 043401
doi: 10.1103/PhysRevLett.124.043401

DR of H_3^+

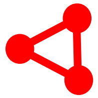

3 atoms

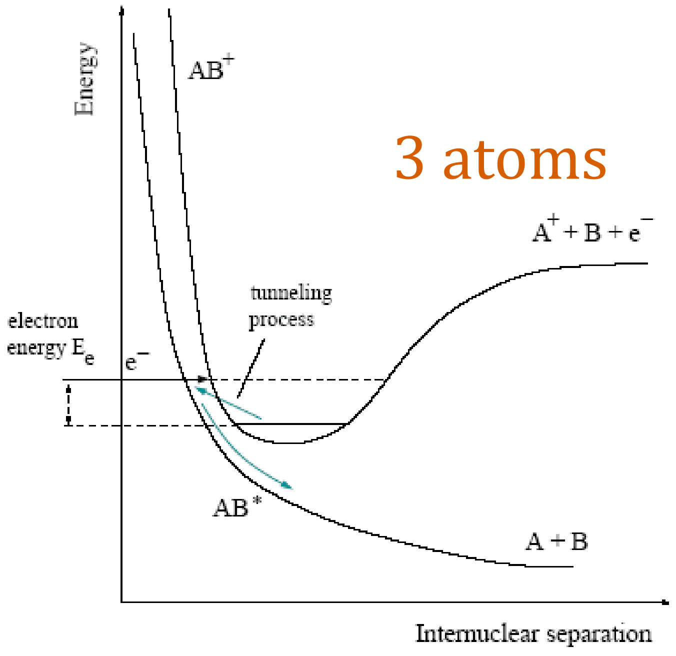

Figure 4.3: *Sketch of tunneling mode dissociative recombination.*

Electron capture via Jahn-Teller coupling of electronic and ro-vibrational motion

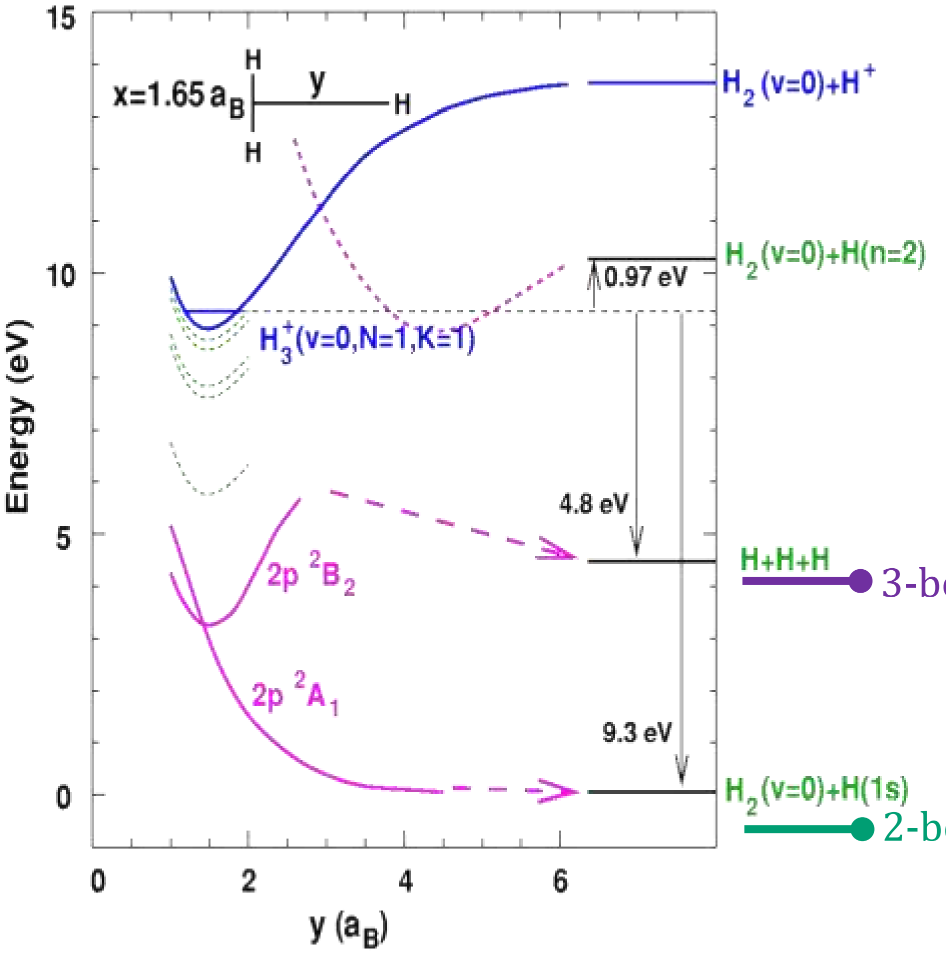

3-body decay

2-body decay

DR of H_3^+

In previous years more than 25 experimental studies resulted in very different values.

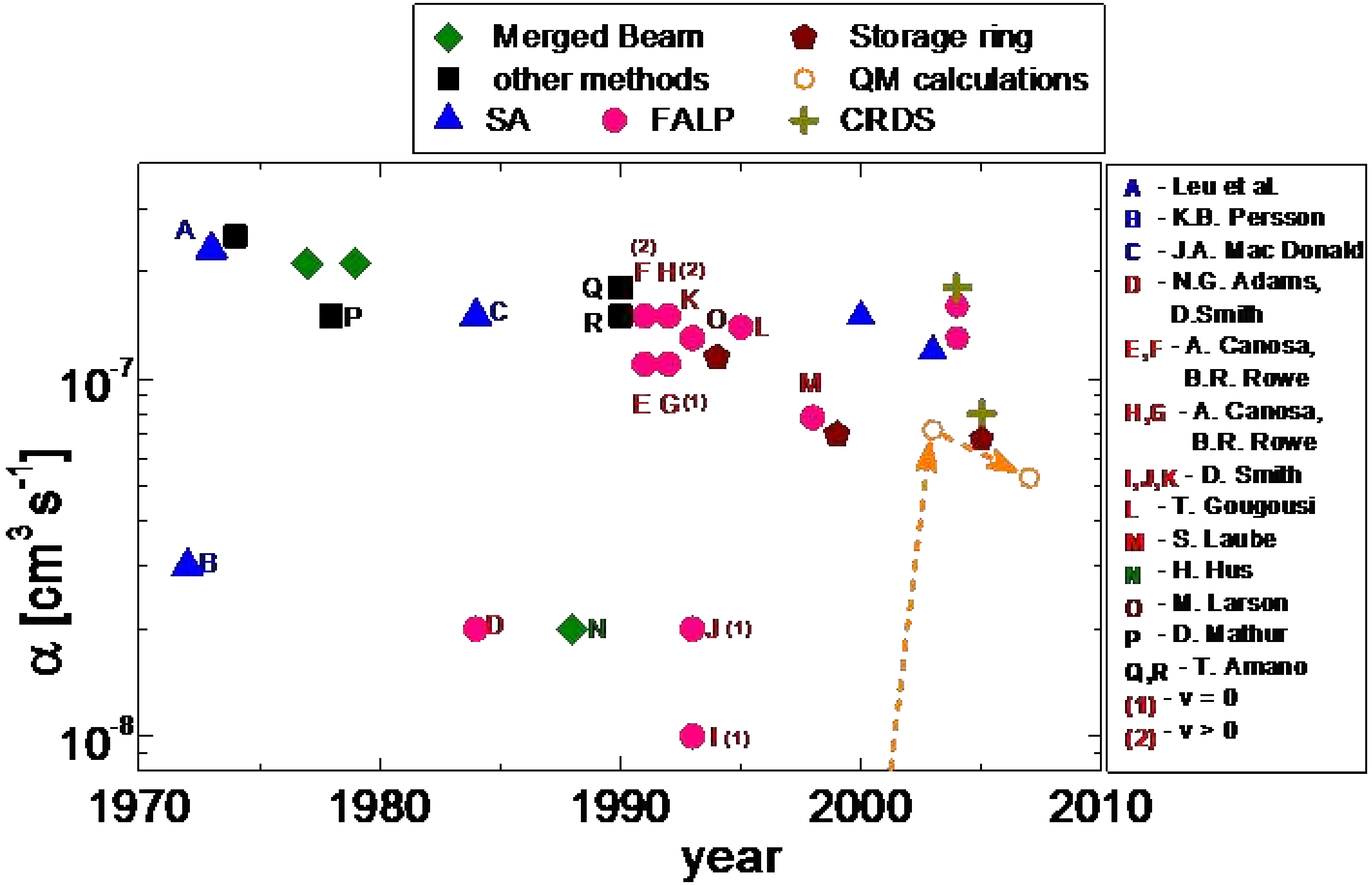

DR experiments 40 – 300 K, 100 – 10k Pa

AISA

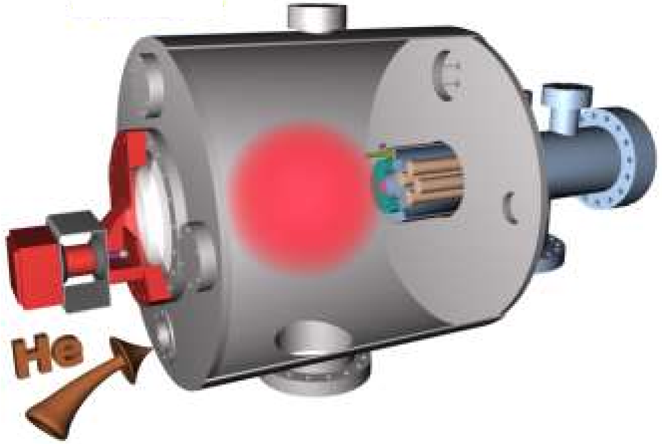

CRDS

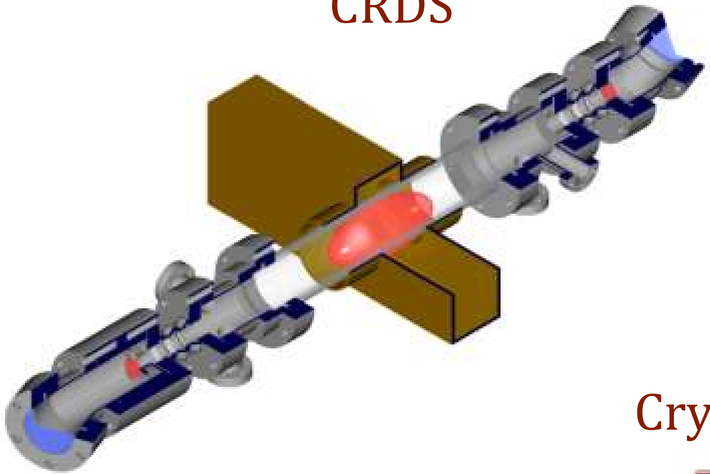

Cryo-SA-CRDS

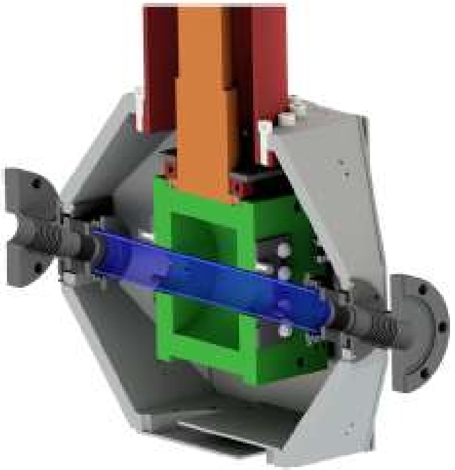

FALP

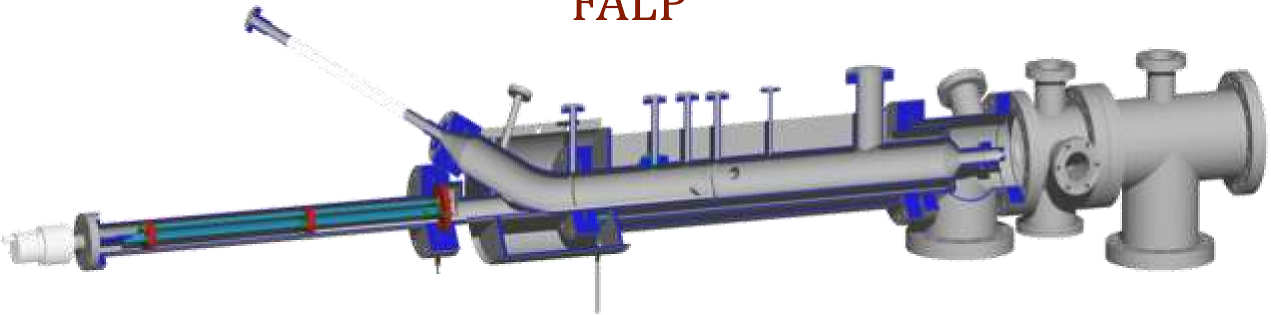

DR of H_3^+

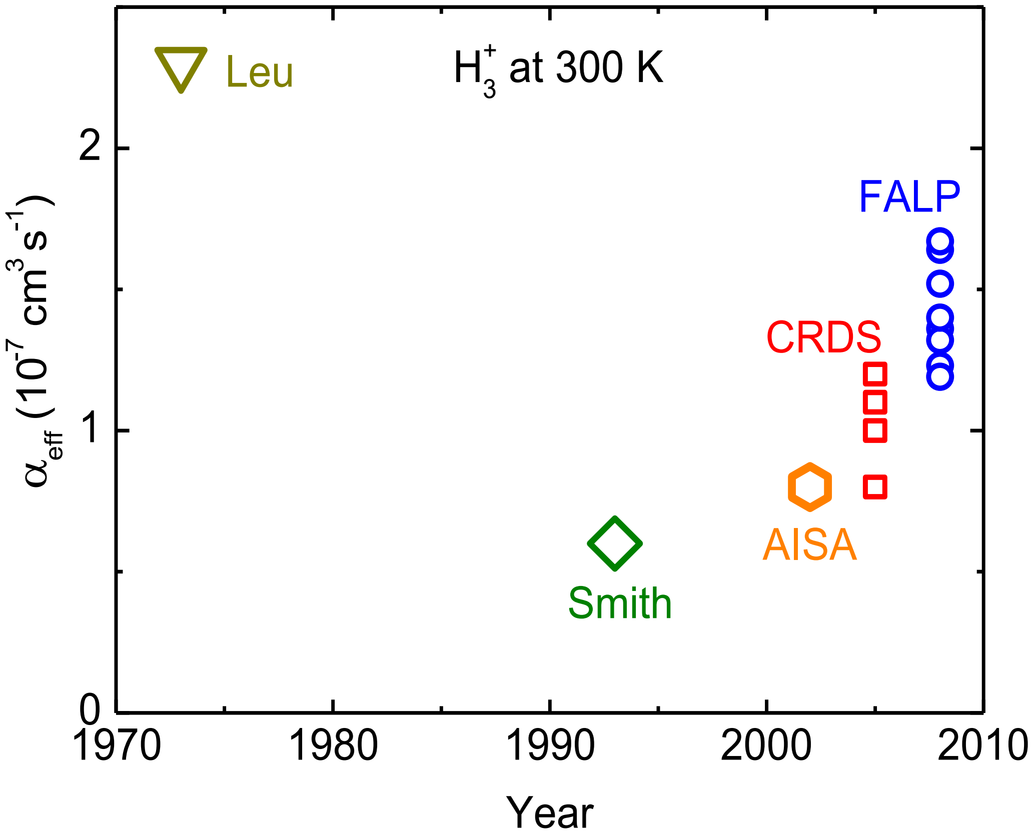

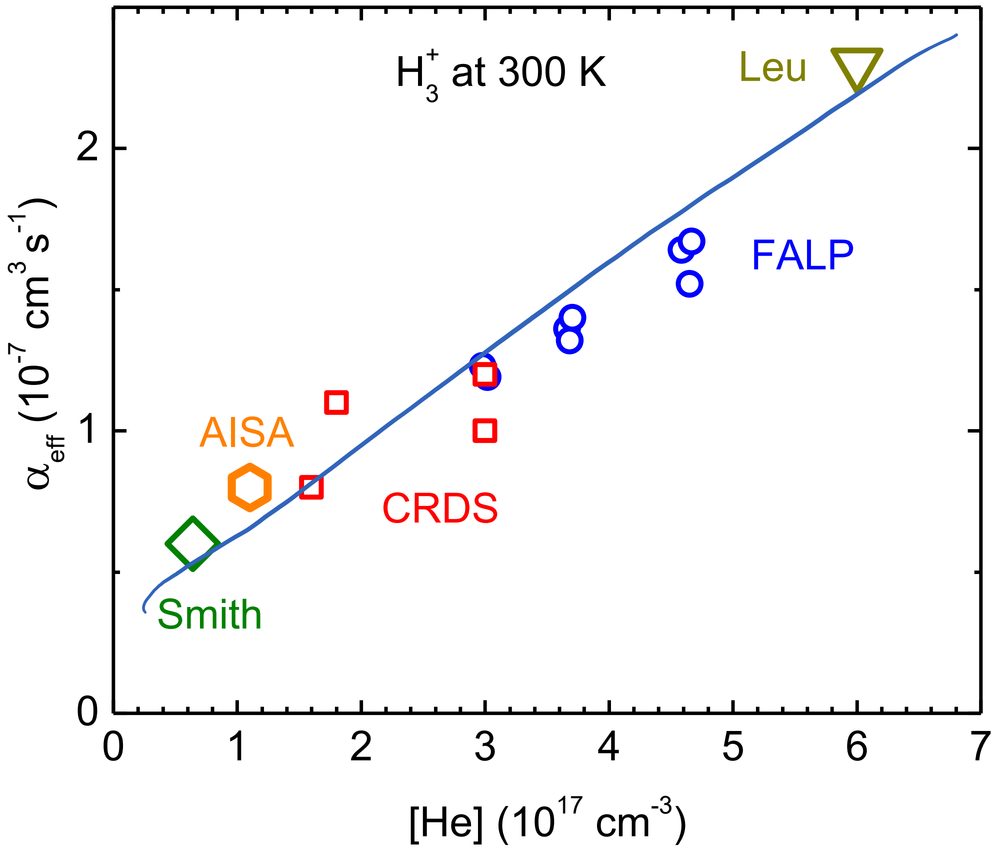

Plašil R. et al. *Int. J. Mass Spectrom.* 218 (2002) 105.
Glosík J. et al. *J. Phys.: Conf. Ser.* 4 (2005) 104.

Macko P. et al. *Int. J. Mass Spectrom.* 233 (2004) 299.
Glosík J. et al. *Phys. Rev. A* 79 (2009) 052707.

Ternary recombination of positive ions

$$\mathrm{H}_3^+ + e^- \underset{\tau_{\mathrm{autoioniz.}}}{\overset{\alpha_{\mathrm{formation}}}{\rightleftarrows}} \mathrm{H}_3^{**} \underset{k_{\mathrm{He}}\cdot[\mathrm{He}]}{\overset{k_{\mathrm{H}_2}\cdot[\mathrm{H}_2]}{\rightrightarrows}} \mathrm{H}_2 + \mathrm{H}\ (\mathrm{H} + \mathrm{H} + \mathrm{H})$$

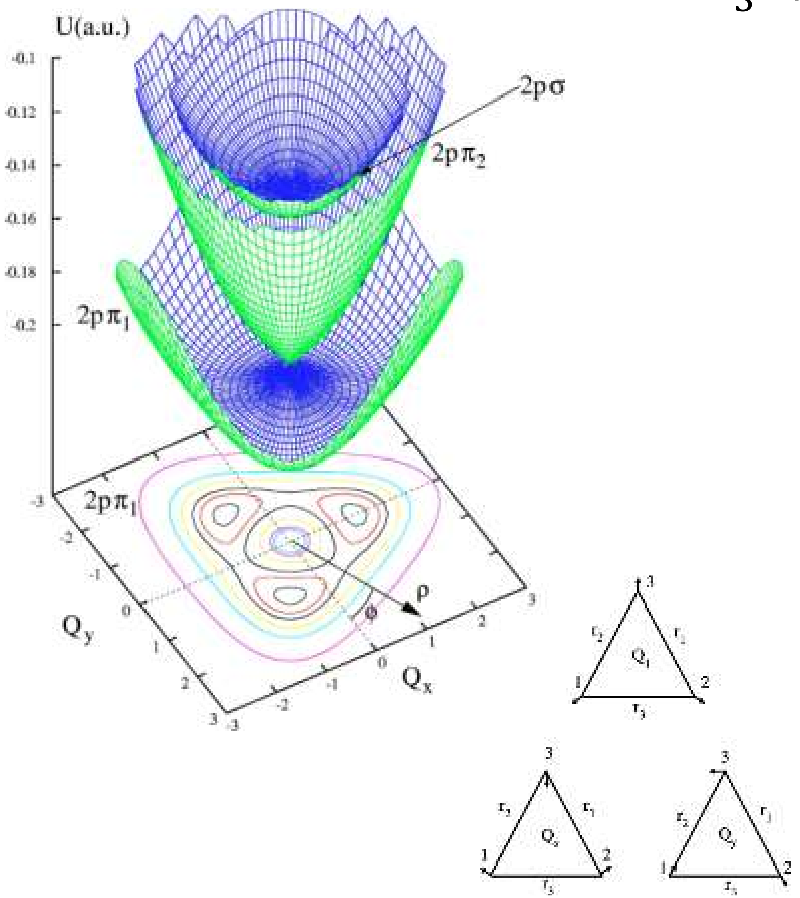

$\tau_{\mathrm{para}} \approx 100$ ps

$\tau_{\mathrm{ortho}} \approx 1$ ps

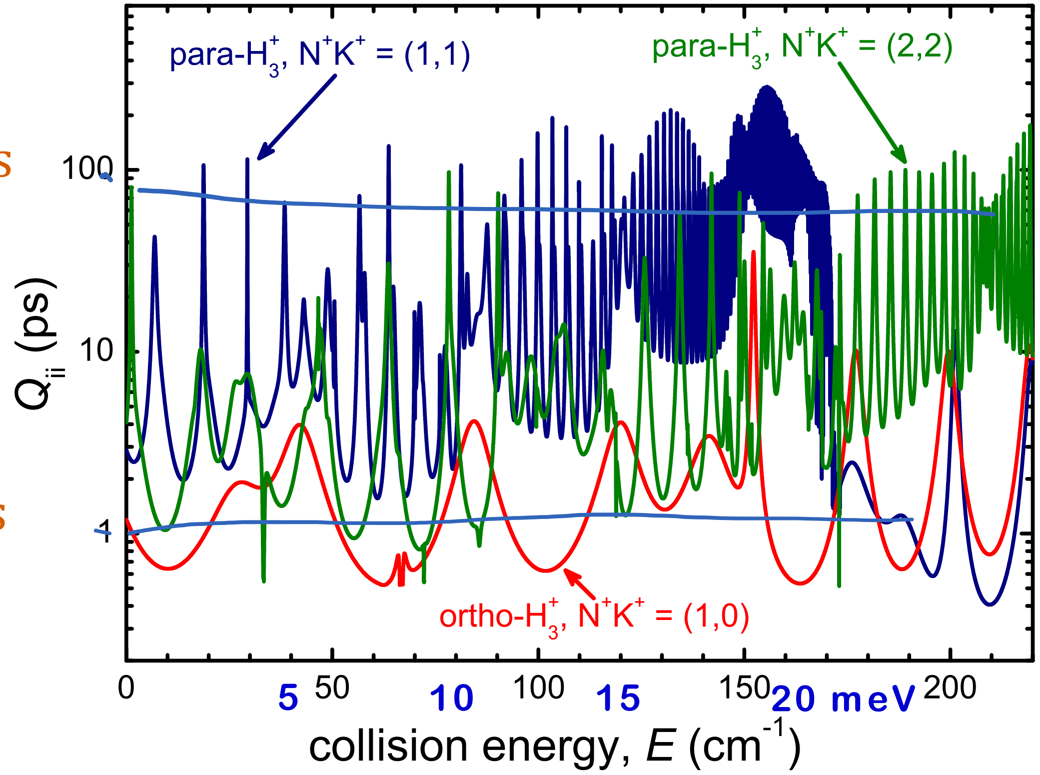

Kokoouline V. and Greene Ch. *Phys. Rev. A* 68 (2003) 012703.
doi: 10.1103/PhysRevA.68.012703

Glosík J. et al. *Phys. Rev. A* 79 (2009) 052707.
doi: 10.1103/PhysRevA.79.052707

DR of H_3^+

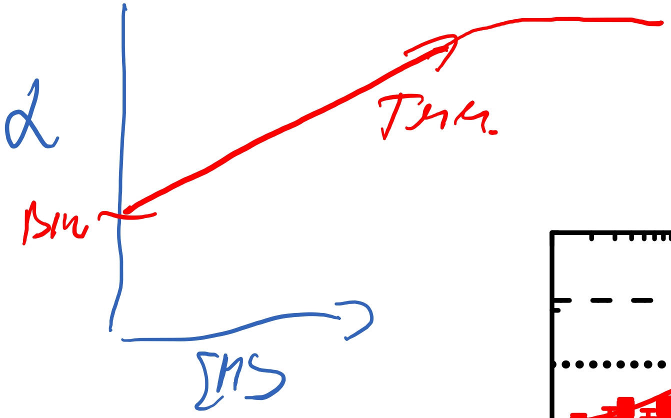

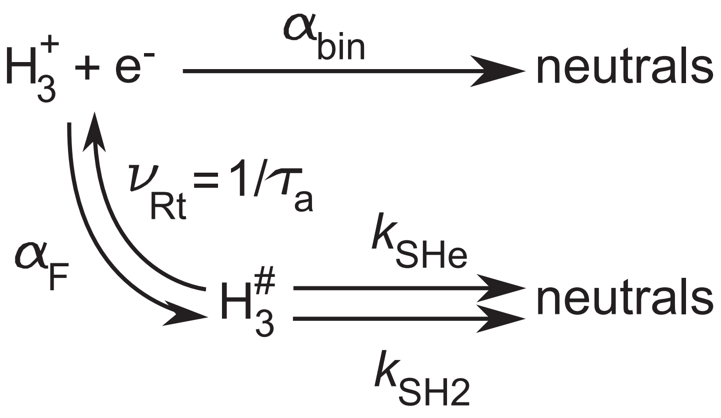

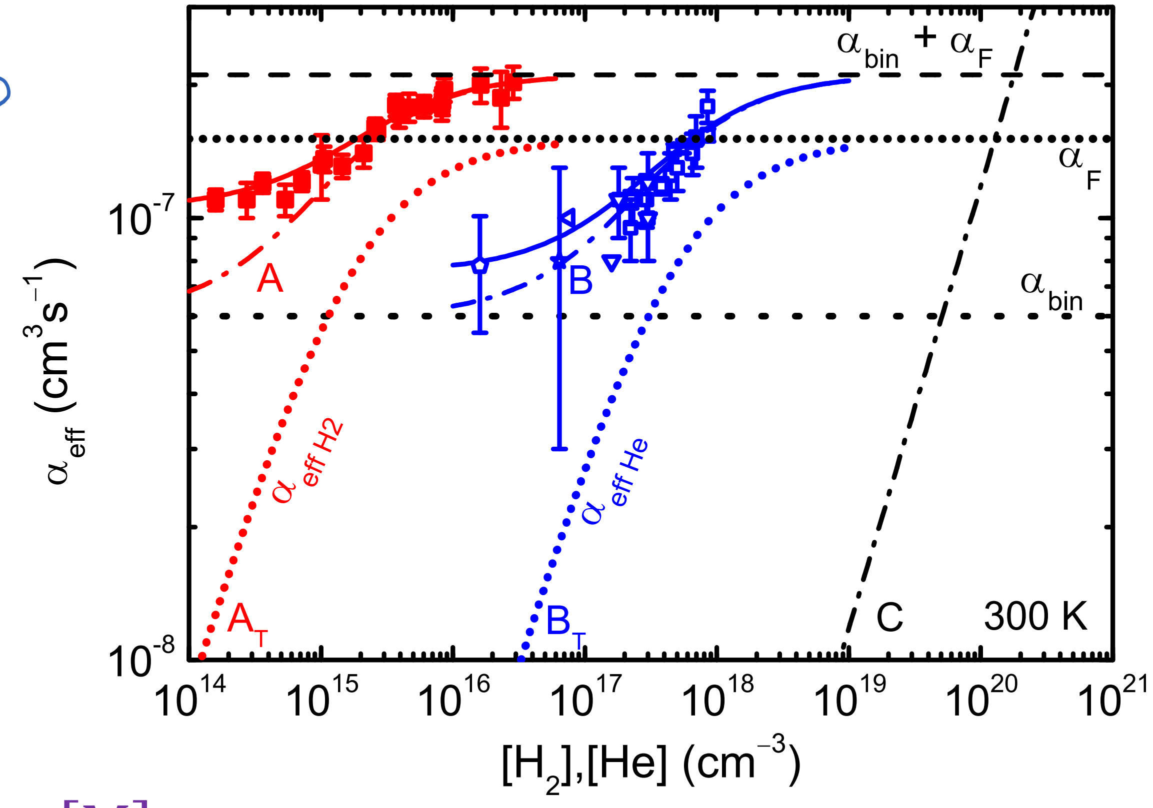

$$\alpha_{\text{eff-bin}} = \alpha_{\text{bin}} + \alpha_{\text{formation}} \frac{k_{\text{sM}}[\text{M}]}{1/\tau_{\text{a}} + k_{\text{sM}}[\text{M}]}$$

Dohnal P. et al. *Phys. Rev. A* 90 (2014) 042708.
doi: 10.1103/PhysRevA.90.042708

Binary DR of para/ortho H_3^+

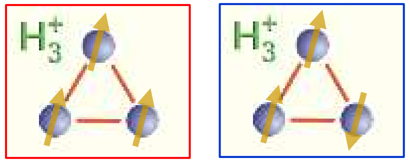

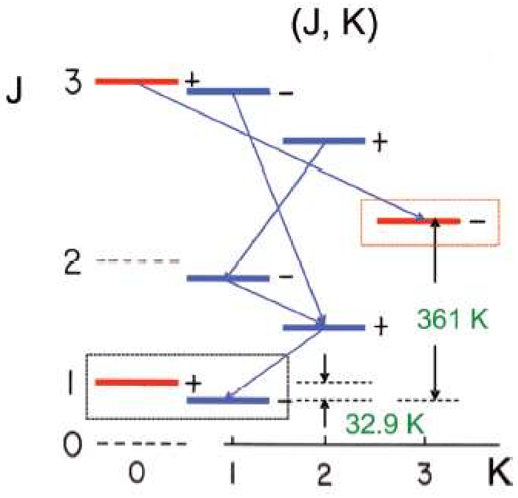

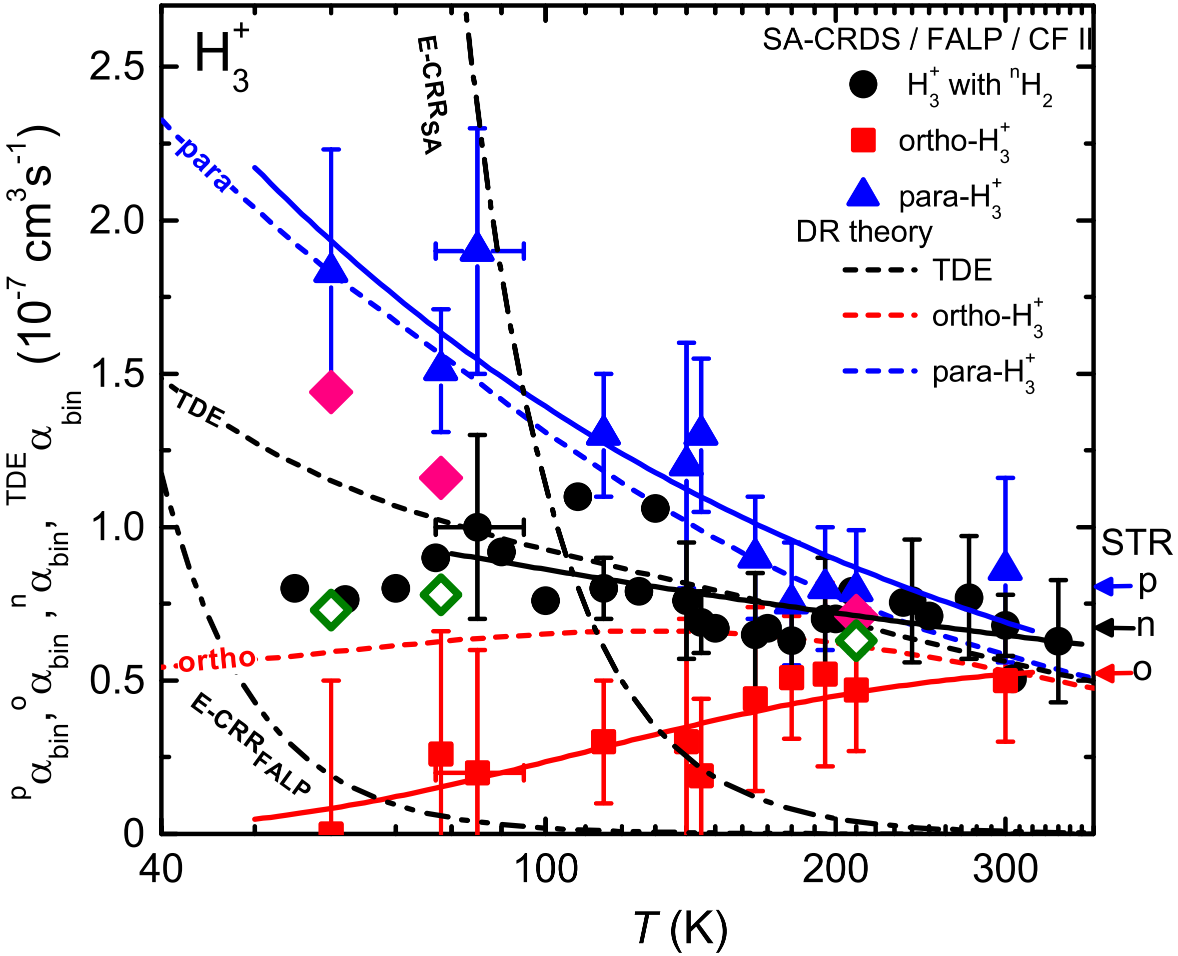

Hejduk M. *J. Chem. Phys.* 143 (2015) 044303
doi: 10.1063/1.4927094